ARTICLE

$Li_{12}Si_{60}H_{60}$ Fullerene Composite: A Promising Hydrogen Storage Medium

Jianhui Lan, Dapeng Cao,* and Wenchuan Wang

Division of Molecular and Materials Simulation, Key Lab for Nanomaterials, Ministry of Education, Beijing University of Chemical Technology, P.R. China

ABSTRACT By using the first-principles DFT calculations, we design a novel hydrogen storage material, $Li_{12}Si_{60}H_{60}$ composite, and validate its geometric stability. It is found that the adsorbed Li atoms do not cluster on the $Si_{60}H_{60}$ fullerene unlike other metals such as Ti, owing to the relatively low Li—Li binding energy and the inhibition of Si—H bonds. Our results show that the Li-doping enhances the hydrogen adsorption ability of $Si_{60}H_{60}$ significantly, owing to the charge transfer from the doped Li atoms to the host material and the polarization of the adsorbed H_2 molecules. By combining the first-principles calculation and grand canonical Monte Carlo simulation, we further investigate the hydrogen storage capacity of the simulation-synthesized exohedral $Li_{12}Si_{60}H_{60}$ composite at $T = 77$ K. As the vdW gap (*i.e.*, the separation between the surfaces of two $Li_{12}Si_{60}H_{60}$ fullerenes) is equal to 8.2 Å, the total hydrogen uptake of the square-arranged $Li_{12}Si_{60}H_{60}$ array reaches 12.83 wt % at $p = 10$ MPa, while the excess hydrogen uptake shows a maximum of 7.46 wt % at $p = 6$ MPa. Impressively, at $T = 298$ K and $p = 10$ MPa, the $Li_{12}Si_{60}H_{60}$ array still exhibits a total hydrogen uptake of 3.88 wt % at the vdW gap of 8.2 Å. These results clearly indicate that the composite, $Li_{12}Si_{60}H_{60}$ fullerene, is a promising candidate for hydrogen storage.

KEYWORDS: hydrogen storage · Li-doped silicon-fullerene · first-principles calculation · grand canonical Monte Carlo simulation · simulating synthesis of materials

Nowadays, the lack of efficient hydrogen storage media is one of the great challenges for hydrogen application in mobile industry. An ideal hydrogen storage material needs to meet several requirements for industrial applications: high capacities, fast kinetics, and proper thermodynamics conditions under which quick adsorption and desorption are readily accessible for hydrogen. However, almost no materials can meet all the requirements so far. It is well-known that the carbon nanotube (CNT) is not an ideal hydrogen storage material because of its poor performance at room temperature. Schlapbach *et al.* believed that it is difficult for carbon materials to achieve a high hydrogen storage capacity unless they hold an extremely high specific surface area (SSA).[1] Cao *et al.* designed a carbonaceous inverse opal material with extremely high BET SSA of 4200 m^2/g and found that this material exhibits a hydrogen uptake of 5.9 wt % at $p = 30$ MPa and room temperature.[2] Schimmel *et al.* explored hydrogen adsorption in carbon nanotube, carbon fibers, and coals and reported that the adsorbed hydrogen only reaches 2 wt % at low temperature.[3] Ansón *et al.* investigated the adsorption of hydrogen in a single-walled carbon nanotube by using three different adsorption techniques, and their results show that the highest capacity does not exceed 0.5 wt % at $p = 20$ bar and room temperature.[4] However, doping metal atoms such as alkali or transition metals (TMs) to carbon-based porous materials, such as CNTs and fullerene, opens a new strategy for hydrogen storage research recently.[5−14] It is found that doping carbon-based materials with some metals can enhance the hydrogen storage capacity significantly, owing to the strong binding energy between H_2 and the doped metal atom. This strong binding energy is mainly attributed to the charge transfer mechanism from the doped metal atoms to the host material. The targeted metals mainly include some light metals like Li, as well as some transition metals in the fourth cycle of the periodic table of elements, such as Ti and Sc. This new strategy is a great advance and makes it possible to design novel hydrogen storage materials that may meet these requirements for industry applications.

Chen *et al.* reported in 1999 that Li- or Pt-doped CNTs can improve hydrogen uptakes significantly compared to nondoped CNTs.[5] Froudakis *et al.* theoretically investigated the nature of interaction between H_2 and alkali-metal-doped CNTs.[6] They believed that the strong binding energy between H_2 and the doped metal atom is induced by

*Address correspondence to caodp@mail.buct.edu.cn.

Received for review July 21, 2009 and accepted September 13, 2009.

Published online September 17, 2009. 10.1021/nn900842j CCC: $40.75

the charge transfer from the alkali metal to the tube which polarizes the adsorbed H_2 molecule. In addition, Ti- and Sc-coated CNTs and fullerenes were also found to exhibit high hydrogen storage capacities up to 8 wt % with a binding energy of about 0.5 eV/H_2 molecule.[10−13] Subsequently, other researchers proved that Ti atoms prefer forming clusters on the C_{60} cage rather than decorating the 12 pentagonal faces.[14] This clustering tendency of the doped Ti atoms makes $Ti_{12}C_{60}$ unsuitable for storing H_2, because its capacity is not higher than 3 wt %. It should be mentioned that most of the research interests in the past were focused on the carbon-based porous materials, while novel materials composed of silicon and other elements may also be promising adsorbents for hydrogen storage as found recently. Ishihara *et al*. experimentally prepared a Si−carbon nanotube composite which is mainly composed of CNTs-coated Si particles, and found that this material shows a relatively large hydrogen uptake (2.5 wt %) at $T = 10$ MPa and $p = 283$ K.[15] Wu *et al*. studied the pillared Li-dispersed boron carbide nanotubes by density functional methods (DFT). Their work indicated that these materials can store hydrogen as much as higher than 6.0 wt %, and boron substitution in CNTs greatly enhances the binding energy of Li atom to nanotube and prevents the Li clustering at high Li-doping concentration.[16] Our previous work also indicated that silicon nanotubes exceed the corresponding isodiameter CNT in hydrogen storage significantly.[17] Lee *et al*. prepared a series of aligned Li-dispersed silicon nanotubes, and reported that these materials exhibit 2-fold increase of H_2 uptake (0.29 wt %) compared to the nondoped ones (0.15 wt %) at 77 K and 4.5 MPa.[18] Most recently, the Si-based fullerene structures were also reported to be possibly suitable hydrogen adsorbents. Karttunen *et al*. predicted a family of stable Ih-symmetric polysilane nanostructures including $Si_{20}H_{20}$, $Si_{80}H_{80}$, and larger structures with DFT calculations.[19] Zhang *et al*. studied hydrogen adsorption in a single $Si_{60}H_{60}$ cage with DFT methods and found that 58 H_2 could be stored in this structure, corresponding to hydrogen capacity of 9.48 wt %.[20] Barman *et al*. predicted that Ti-coated $P_{10}Si_{50}H_{50}$ can adsorb 80 H_2 molecules, corresponding to H_2 uptake of 6 wt %.[21] In contrast, the Ti atoms doped on $Si_{60}H_{60}$ still tend to cluster together, and this degrades their hydrogen storage capacity.

In this work, we use a molecular simulation method to design a novel hydrogen storage material, exohedral $Li_{12}Si_{60}H_{60}$ composite, which possesses not only outstanding hydrogen uptake but also excellent structural stability. To validate the feasibility of the composite material, we need to address the following three issues. First, is the simulation-synthesized $Li_{12}Si_{60}H_{60}$ composite stable enough for practical applications?

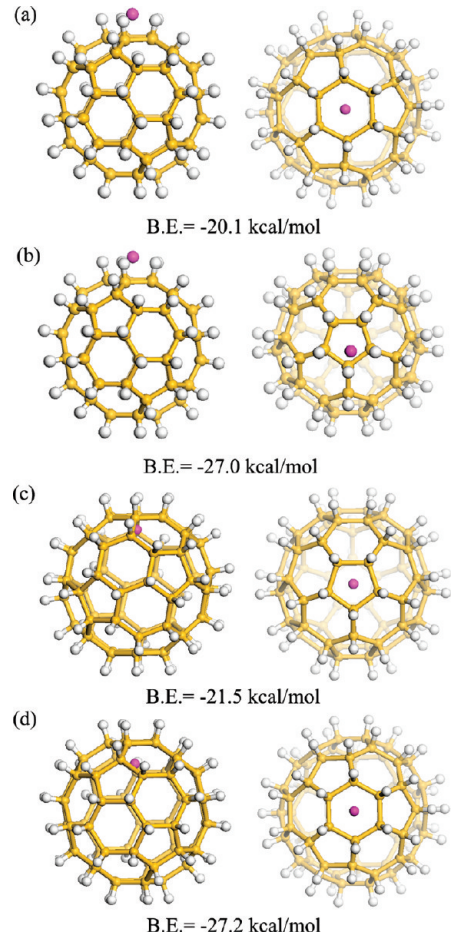

Figure 1. Possible adsorption sites of a single Li atom inside and outside surfaces of the $Si_{60}H_{60}$ fullerene, respectively. The left panel shows the side view and the right shows the top view. White, yellow, and pink denote H, Si, and Li, respectively.

Second, do the coated Li atoms tend to form clusters when adsorbed on the $Si_{60}H_{60}$ fullerene? Third, how does the exohedral functionalization with Li-doping enhance the hydrogen storage capacity of $Si_{60}H_{60}$? To answer these questions, a multiscale theoretical method, which combines the first-principles DFT calculation and the grand canonical Monte Carlo (GCMC) simulation, was adopted.

RESULTS AND DISCUSSION

First of all, we used the first-principles calculations to design the $Li_{12}Si_{60}H_{60}$ composite and investigate its structural stability. The initial procedure for the design of the Li-coated $Si_{60}H_{60}$ composite is to study the site preference of a single Li atom. When a single Li atom resides outside $Si_{60}H_{60}$, it prefers to be adsorbed at the pentagonal site with a binding energy of −27.0 kcal/mol, which is significantly higher than −20.1 kcal/mol at the hexagonal site (see Figure 1). At the pentagonal site, the distance between the doped Li atom and its nearest H atom is only 1.80 Å, while at the hexagonal site this value is about 2.99 Å. On the contrary, inside the $Si_{60}H_{60}$ surface, the hexagonal site is more prefer-

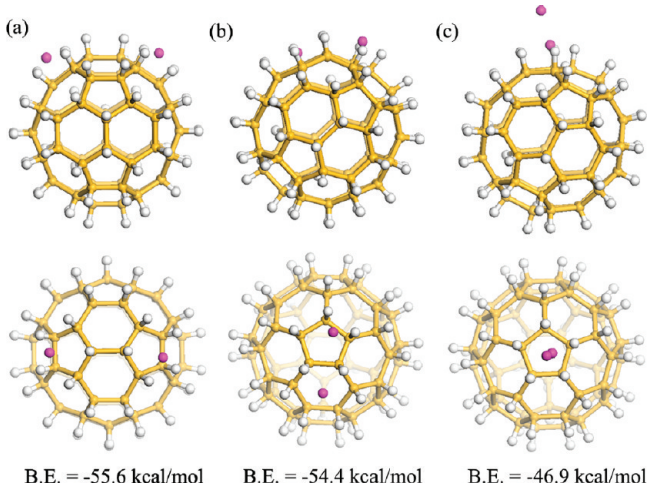

Figure 2. Possible adsorption sites for two Li atoms at the outer surface of the $Si_{60}H_{60}$ fullerene: (a) on two pentagonal sites, (b) on two neighboring pentagonal and hexagonal sites, (c) on a single pentagonal site. The upper and bottom panels show the side and top views, respectively. White, yellow, and pink denote H, Si and Li, respectively.

able for Li than the pentagonal one. The calculated binding energy for a Li atom adsorbed on the inner hexagonal site is about −27.2 kcal/mol, and that for the inner pentagonal site is just −21.5 kcal/mol. Although the binding energies for Li outside and inside $Si_{60}H_{60}$ fullerene are comparable, occupation of Li atoms inside the surface is difficult because of the limitation of pore size in the $Si_{60}H_{60}$ fullerene. Therefore, in the following work, we just took into account Li adsorption on the outer surface of the $Si_{60}H_{60}$ fullerene.

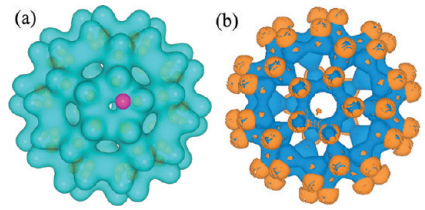

Figure 3. 3D distribution of (a) electron density at the isosurface level of 0.016 au and (b) Laplacian of electron density at the isosurface level of 0.047 au for the $LiSi_{60}H_{60}$ system, where a Li atom is deposited at the pentagonal site. In panel b, charge concentrations are colored in orange and charge depletions are colored in blue.

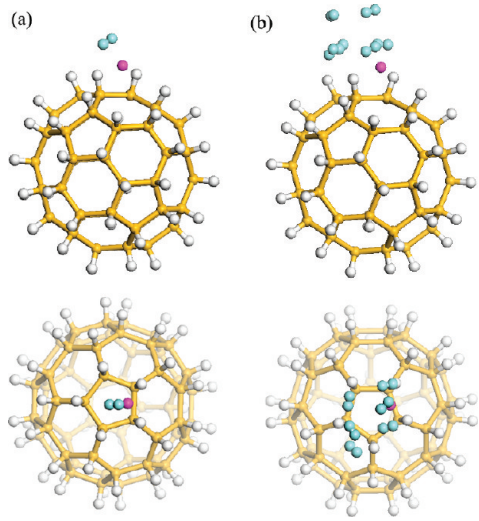

Figure 4. Adsorption of one and six H_2 molecules at the exohedral $LiSi_{60}H_{60}$ composite. The upper and bottom panels give the side and top views, respectively. White, yellow and pink represents H, Si and Li, while blue represents the adsorbed H_2 molecules.

Figure 2 displays the optimized adsorption positions for two Li atoms on the $Si_{60}H_{60}$ surface. Our first-principles calculation confirms that the Li atoms do not cluster when they are bound to the exohedral $Si_{60}H_{60}$ fullerene. Among the several coadsorption modes, dispersion of each Li adatom to the pentagonal site is the most favorable one with a coadsorption energy of −55.6 kcal/mol. The second favorable coadsorption mode is that one Li atom locates at a pentagonal site and the other locates at its neighboring hexagonal site with a binding energy of −54.4 kcal.mol. Owing to the steric effect, occupying one pentagonal site with two Li atoms is the most impossible coadsorption mode with a binding energy of −46.9 kcal/mol. In fact, the reasons that we can not observe Li-clustering phenomenon at the $Si_{60}H_{60}$ material are, first, the binding energy between Li atoms is relatively lower than that for TMs such as Ti and Ni; second, the existence of Si−H bond inhibits the clustering tendency of Li atoms. From the calculations above, it is suggested that the $Si_{60}H_{60}$ can at least load 12 Li atoms stably in energy, forming $Li_{12}Si_{60}H_{60}$ composite with each pentagon face loading one Li atom.

To further probe the interaction nature between the doped Li atom and the host material, we analyzed the Bader charge of the doped Li atom by using the $LiSi_{60}H_{60}$ complex in Figure 1b as a representative. It is found that the exohedrally adsorbed Li atom is positively charged with a quantity of $+1|e|$, either at the hexagonal or pentagonal sites. These results are in agreement with the electron density and its Laplacian for $LiSi_{60}H_{60}$, as shown in Figure 3. Because of the charge transfer from the Li atom to the host material, the valence charge around the Li atom is not visible in Figure 3a. As is well-known, the Laplacian of an electron density recovers the shell structure of an atom. A negative Laplacian represents the concentration of the negative charge, while a positive Laplacian denotes the depletion of the negative charge. From Figure 3a,b, the highly covalent Si−Si and Si−H bonds and the ionic nature of the interactions between the capped Li atom and Si, H atoms are clearly visualized.

After the structure of the $Li_{12}Si_{60}H_{60}$ composite is determined, we intend to discuss the mechanism, which the exohedral functionalization with Li-doping enhances the hydrogen adsorption of $Si_{60}H_{60}$. It is well-known that the pure $Si_{60}H_{60}$ fullerene shows very low affinity to H_2. Based on our calculations, the binding energies for H_2 at the hexagonal site outside and inside the cage are −0.55 and −0.74 kcal/mol, respectively. These data indicate that the pure $Si_{60}H_{60}$ fullerene

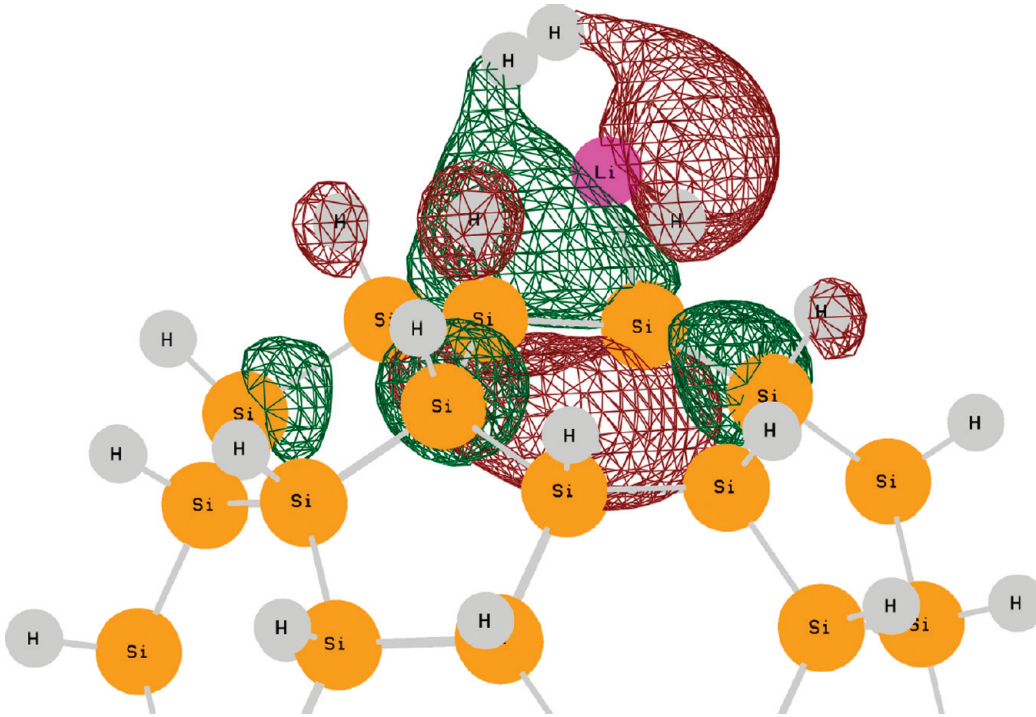

Figure 5. Highest occupied molecular orbital (HOMO) for a H_2 molecule adsorbed at the $LiSi_{60}H_{60}$ composite, where the Li atom is doped on the outer pentagonal site.

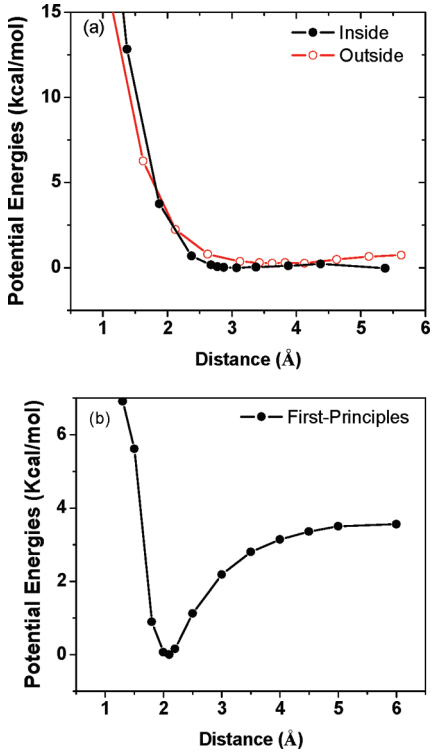

Figure 6. (a) Calculated potential energies for H_2 interaction with the $Si_{60}H_{60}$ fullerene, where H_2 keeps away from the center of a hexatomic ring inside and outside, respectively, with its axis vertical to the surface. The abscissa axis denotes the distance between the hexatomic ring center and the center of H_2. Here, the potential energies are relative to the minimum of the inside case. (b) Calculated potential energies for H_2 interaction with a Li cation adsorbed on the outer pentagonal site of the $Si_{60}H_{60}$ fullerene.

is not suitable for high-capacity hydrogen storage. However, the Li-coated $Li_{12}Si_{60}H_{60}$ composite is a promising hydrogen storage material, because the doped Li atoms greatly enhance the composite affinity toward hydrogen. To investigate the interaction between H_2 and the Li cation doped on the $Si_{60}H_{60}$ exohedrally, we consequently studied the adsorption of a single H_2 molecule at the representative $LiSi_{60}H_{60}$ cage (see Figure 4 (a)) to reduce the computational cost. In the $Li_{12}Si_{60}H_{60}$ composite, the doped Li atoms are far from each other, therefore, using $LiSi_{60}H_{60}$ as the prototype can yield equivalent results. In the ground-state configuration, our results show that the first H_2 molecule is adsorbed in the molecule form with a bond length of 0.755 Å, and the distance between the Li cation and each H atom is about 2.08 Å. The calculated binding energy for the $H_2-LiSi_{60}H_{60}$ interaction is about −4.84 kcal/mol, suggesting that the doped Li cation enhances the H_2 binding energy significantly. It should be pointed out that the adsorbed H_2 molecule is polarized in the ground state, with the left H atom of H_2 in Figure 4a charged by +0.01 |e| and the other by −0.02 |e|. Figure 5 shows

TABLE 1. Parameters of the Morse Potential Used to Describe the Interaction between a H_2 Molecule and the $Li_{12}Si_{60}H_{60}$ Composite Material[a]

parameters	H_A-H	H_A-Si	H_A-Li
D (kcal/mol)	0.0158	0.055	1.820
γ	12.018	12.020	6.283
r_e (Å)	3.285	3.722	2.080

[a] H_A denotes the H atom in H_2, and Si, H, and Li denote the corresponding atom types in $Li_{12}Si_{60}H_{60}$.

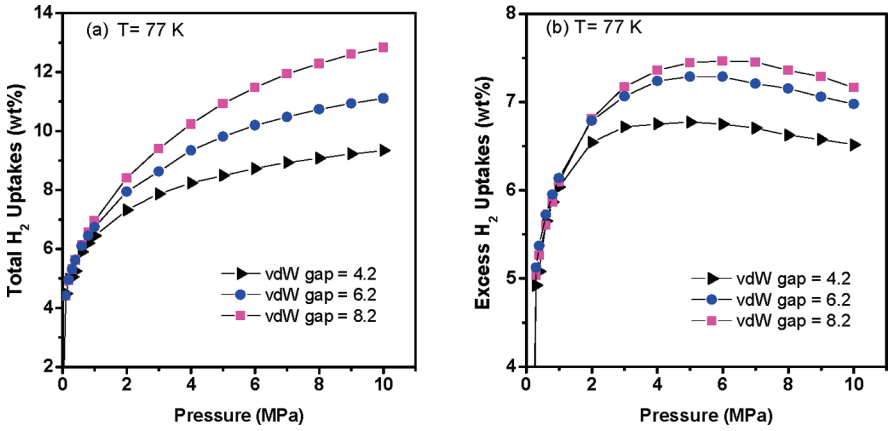

Figure 7. Computed H_2 adsorption isotherms in the $Li_{12}Si_{60}H_{60}$ array at $T = 77$ K: (a) total gravimetric isotherms; (b) excess gravimetric isotherms. vdW gap denotes the separation between the surfaces of two neighboring $Li_{12}Si_{60}H_{60}$ units.

the isosurface plot for the highest occupied molecular orbital (HOMO) of the system studied above. In the HOMO, mainly Li $3P_x$ orbital participates in the hybridization with the coniugated π orbital of the Si atoms in the pentagon and H 2s orbital of H_2. It is noticed that during the hybridization of the atomic orbital, Li 1s electron has been provoked to $3P_x$ orbital due to necessity of hybridization. Another important point we are concerned about is the maximum number of H_2 molecules that can be bound to a Li cation. Therefore, we added the H_2 molecules around the doped Li cation from different directions continually and optimized their adsorption positions without any constraints. It is found that as the number of H_2 increases, the binding energies decrease accordingly. The calculated binding energy for the second H_2 molecule adsorbed at the Li cation is about −2.16 kcal/mol and those for the third, fourth, fifth, and sixth are −1.66, −1.49, −1.33, and −1.12 kcal/mol, respectively. As shown in Figure 4b, the adsorbed H_2 molecules form two obvious layers.

In the investigations above, we used the first-principles calculations to obtain the interactions between H_2 and the $Si_{60}H_{60}$ fullerene as well as the doped Li atom. Next, the obtained interaction energies were fitted to the Morse potential (see eq 1) to achieve the force field parameters for the interactions such as H−Si and H−Li. Figure 6a shows the calculated potential energies for H_2 adsorption inside and outside the $Si_{60}H_{60}$ fullerene, respectively, where the potential energies were obtained by making a H_2 molecule pass through a hexatomic ring with its axis vertical to the plane. Figure 6b gives the potential energies for H_2 interaction with a Li cation doped at an outer pentagonal site, where the H_2−Li interaction mode is shown in Figure 4a. The obtained potential energies were then fitted to the Morse potential, given by

$$U_i = D[x^2 - 2x], \quad x = \exp\left(-\frac{\gamma}{2}\left(\frac{r_i}{r_e} - 1\right)\right) \qquad (1)$$

where r_i is the interaction distance in Å. D, γ, and r_e denote the well depth, the stiffness (force constant), and the equilibrium bond distance, respectively. Here, the hydrogen molecule was treated as a diatomic molecule. Table 1 lists the fitted force field parameters for the interactions between H_2 and the Li-coated $Si_{60}H_{60}$ material.

Using these data, GCMC simulations were finally performed to predict the hydrogen storage capacities of the $Li_{12}Si_{60}H_{60}$ composite at $T = 77$ K. Figure 7 presents the calculated total and excess gravimetric isotherms of hydrogen adsorption in the square-arranged $Li_{12}Si_{60}H_{60}$ array at $T = 77$ K and different van de Waals (vdW) gaps, where the vdW gap is defined as the separation between the surfaces of two neighboring $Li_{12}Si_{60}H_{60}$ units. The snapshots for hydrogen storage in the array with the vdW gap equal to 8.2 Å at $T = 77$ K and 10 MPa are also shown in Figure 8. Our GCMC results indicate that, as the vdW gap is equal to 8.2 Å, the total gravimetric hydrogen uptakes in the $Li_{12}Si_{60}H_{60}$ array achieve 6.95, 10.94, and 12.83 wt % at $T = 77$ K and $p = 1$, 5, and 10 MPa, respectively. This superior hydrogen storage performance can be attributed to the enhancement effect of Li-doping. As the vdW gap decreases to 6.2 and

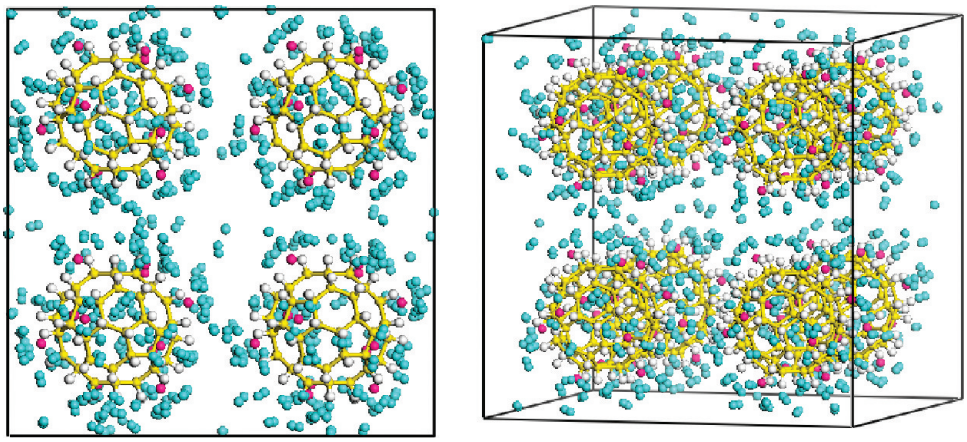

Figure 8. Snapshots for hydrogen adsorption in the $Li_{12}Si_{60}H_{60}$ array at $T = 77$ K and $p = 10$ MPa with the vdW gap of 8.2 Å. The simulation box contains eight $Li_{12}Si_{60}H_{60}$ units in the GCMC simulations. Left panel, top view; right panel, side view.

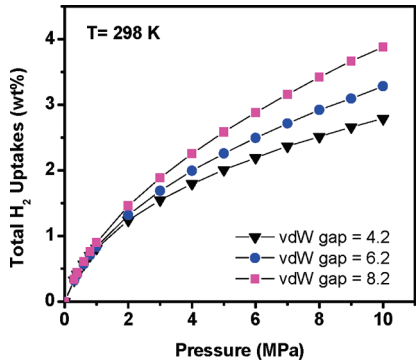

Figure 9. Computed H_2 adsorption isotherms in the $Li_{12}Si_{60}H_{60}$ array at $T = 298$ K.

4.2 Å, the $Li_{12}Si_{60}H_{60}$ array still exhibits high hydrogen uptakes of 11.11 and 9.34 wt % at $T = 77$ K and $p = 10$ MPa, respectively. It is noted from our calculations that the adsorbed H_2 molecules mainly distribute outside the $Li_{12}Si_{60}H_{60}$ cage due to the strong binding energy between H_2 and Li cations doped on the outer surface. Even at $p = 10$ MPa, the number of H_2 molecules stored inside the sphere is still no more than 4 on average. Figure 7 b shows the excess gravimetric hydrogen uptakes at $T = 77$ K. As the vdW gap equals 8.2 Å, the excess hydrogen uptakes of the $Li_{12}Si_{60}H_{60}$ array show a maximum of 7.46 wt % at 6 MPa. In contrast, when the vdW gap equals 6.2 Å, the $Li_{12}Si_{60}H_{60}$ array displays a comparable excess hydrogen uptake as above. However, as the vdW gap decreases to 4.2 Å, the excess hydrogen uptakes decrease evidently for the steric effect. By comparison, the vdW gap of 8.2 Å gives nearly the highest total and excess hydrogen capacities for the $Li_{12}Si_{60}H_{60}$ array. It can be found from Figure 8 that the adsorbed H_2 molecules are mainly bound to the Li cations, originating from their strong affinity to H_2. Our GCMC simulations indicate that the $Li_{12}Si_{60}H_{60}$ composite is one of the most promising candidates for hydrogen storage, which gives a comparable hydrogen storage capacity to 3D covalent organic frameworks as reported by experiment[22] and simulations.[23]

For the practical use of hydrogen at room temperature, we also investigated the adsorption capacity of the $Li_{12}Si_{60}H_{60}$ composite at $T = 298$ K. The predicted total gravimetric isotherms for hydrogen adsorption in the $Li_{12}Si_{60}H_{60}$ array are shown in Figure 9. Impressively, at $T = 298$ K the squared-arranged $Li_{12}Si_{60}H_{60}$ array still exhibits good hydrogen storage performance. The amount of H_2 stored in the array is slightly dependent on the vdW gap. At $T = 298$ K and $p = 10$ MPa, the total gravimetric uptakes of hydrogen reach 2.79, 3.57, and 3.88 wt %, corresponding to the vdW gaps of 4.2, 6.2, and 8.2 Å, respectively. As analyzed above, the doped Li atom is the main source of affinity to H_2 in the $Li_{12}Si_{60}H_{60}$ composite. By observing the snapshots of interaction between H_2 and the host material, it is found that at $T = 298$ K and $p = 10$ MPa, each Li atom can attract approximately three hydrogen molecules in the array. In short, the $Li_{12}Si_{60}H_{60}$ composite is a promising hydrogen adsorbent.

CONCLUSIONS

We have used a multiscale theoretical method, which combines the first-principles DFT calculations and the GCMC simulations, to design a novel hydrogen storage composite, $Li_{12}Si_{60}H_{60}$, and further investigate its hydrogen storage capacities. Our simulation results indicate that the $Si_{60}H_{60}$ fullerene can bind with Li atoms strongly with a binding energy of about −27.0 kcal/mol at the outer pentagonal site. This strong interaction energy is attributed to the charge transfer mechanism from Li atoms to the host material. At least 12 Li atoms can be loaded to its 12 pentagon faces exohedrally, forming the $Li_{12}Si_{60}H_{60}$ composite. Impressively, the adsorbed Li atoms do not cluster on the surface of the $Si_{60}H_{60}$ fullerene for the relatively low Li−Li binding energy and the inhibition of Si−H bonds, unlike the cases of Ti-doping on C_{60}, CNTs, and $Si_{60}H_{60}$. The doped Li cations can enhance the hydrogen adsorption ability of $Si_{60}H_{60}$ significantly. Our GCMC results show that the $Li_{12}Si_{60}H_{60}$ array exhibits a maximal excess hydrogen uptake of 7.46 wt % at $p = 6$ MPa and $T = 77$ K at the vdW gap of 8.2 Å, which is comparable to the well-known 3D covalent organic frameworks. Furthermore, the predicted hydrogen adsorption isotherms at $T = 298$ K show that the $Li_{12}Si_{60}H_{60}$ array can store as much as 3.88 wt % of H_2 at the vdW gap of 8.2 Å and $p = 10$ MPa, where each Li atom attracts nearly three H_2 molecules. These results suggest that the composite material, $Li_{12}Si_{60}H_{60}$, is a promising candidate for hydrogen storage. These theoretical results are encouraging and remain also to be further validated in experiment.

COMPUTATIONAL DETAILS

All the first-principles DFT calculations here were carried out by using the Vienna *ab Initio* Simulation Program (VASP).[24,25] The approach implemented in VASP is based on the (finite-temperature) local-density approximation with the free energy as variational quantity and an exact evaluation of the instantaneous electronic ground state at each molecular dynamics (MD) time step. Here, the generalized gradient approximation (GGA) was adopted together with the functional of Perdew and Wang.[26] The interaction between ions and electrons is described by ultrasoft Vanderbilt[27] pseudopotentials (US-PP), as implemented by Kresse and Hafner.[28] The tight convergence of the plane-wave expansion was obtained with an energy cutoff of 240 eV. For energy calculation, the electronic energy was converged to 10^{-4} eV, and the positions of the atoms were allowed to relax until all forces were smaller than 10^{-3} eV/Å^2. For the Li-coated $Si_{60}H_{60}$, a 23 × 23 × 23 Å^3 cubic cell was adopted. The Brillouin zone was sampled at the gamma point with a gamma-centered grid for the large cells used here. The positions of all the atoms

in the supercell were fully relaxed without the symmetry constraint during the geometry optimizations. The binding energy is defined as

$$BE = E(\text{adsorbates/host}) - E(\text{adsorbates}) - E(\text{host}),$$

where E(adsorbates/host), E(adsorbates) and E(host) are the energies of the complex coadsorption species, the separated adsorbates, and the host material, respectively.

By performing first-principles calculations, the potential energies of the adsorbates at the surface of the host material were then obtained. Using the force field parameters derived from the calculated potential energies as input, we performed GCMC simulations to evaluate the hydrogen uptake of the $Li_{12}Si_{60}H_{60}$ composite. During the GCMC simulation, the cubic simulation box consists of eight $Li_{12}Si_{60}H_{60}$ units, which are square-arranged and uniformly spaced. The periodic boundary conditions were applied in all the three dimensions. The cutoff radius is six times the collision diameter of adsorbates. To obtain the relationship between the chemical potential and pressure, the Widom's test particle insertion method in the NVT ensemble was used.[29] The details of the GCMC simulation can be found in our previous works.[17,23,30]

Acknowledgment. This work is supported by NSF of China (20776005, 20736002), National Basic Research Program of China (2007CB209706), Beijing Novel Program (2006B17), NCET Program (NCET-06-0095) and ROCS Foundation (LX2007-02), and Novel Team (IRT0807) from the MOE of China.

REFERENCES AND NOTES

1. Schlapbach, L.; Zuttel, A. Hydrogen-Storage Materials for Mobile Applications. *Nature* **2001**, *414*, 353–358.
2. Cao, D. P.; Feng, P. Y.; Wu, J. Z. Molecular Simulation of Novel Carbonaceous Materials for Hydrogen Storage. *Nano Lett.* **2004**, *4*, 1489–1492.
3. Schimmel, H. G.; Kearley, G. J.; Nijkamp, M. G.; Visser, C. T.; de Jong, K. P.; Mulder, F. M. Hydrogen Adsorption in Carbon Nanostructures: Comparison of Nanotubes, Fibers, and Coals. *Chem.—Eur. J.* **2003**, *9*, 4764–4770.
4. Ansón, A.; Benham, M.; Jagiello, J.; Callejas, M. A.; Benito, A. M.; Maser, W. K.; Züttel, A.; Sudan, P.; Martinez, M. T. Hydrogen Adsorption on a Single-Walled Carbon Nanotube Material: A Comparative Study of Three Different Adsorption Techniques. *Nanotechnology* **2004**, *15*, 1503–1508.
5. Chen, P.; Wu, X.; Liu, J.; Tan, K. L. High H_2 Uptake by Alkali-Doped Carbon Nanotubes Under Ambient Pressure and Moderate Temperatures. *Science* **1999**, *285*, 91–93.
6. Froudakis, G. E. Why Alkali-Metal-Doped Carbon Nanotubes Possess High Hydrogen Uptake. *Nano Lett.* **2001**, *1*, 531–533.
7. Han, S. S.; Goddard III, W. A. Lithium-Doped Metal−Organic Frameworks for Reversible H_2 Storage at Ambient Temperature. *J. Am. Chem. Soc.* **2007**, *129*, 8422–8423.
8. Mavrandonakis, A.; Tylianakis, E.; Stubos, A. K.; Froudakis, G. E. Why Li Doping in MOFs Enhances H_2 Storage Capacity? A Multiscale Theoretical Study. *J. Phys. Chem. C* **2008**, *112*, 7290–7294.
9. Han, S. S.; Goddard, W. A. High H_2 Storage of Hexagonal Metal−Organic Frameworks from First-Principles-Based Grand Canonical Monte Carlo Simulations. *J. Phys. Chem. C* **2008**, *112*, 13431–13436.
10. Zhao, Y. F.; Kim, Y. H.; Dillon, A. C.; Heben, M. J.; Zhang, S. B. Hydrogen Storage in Novel Organometallic Buckyballs. *Phys. Rev. Lett.* **2005**, *94*, 155504.
11. Yildirim, T.; Iniguez, J.; Ciraci, S. Molecular and Dissociative Adsorption of Multiple Hydrogen Molecules on Transition Metal Decorated C_{60}. *Phys. Rev. B* **2005**, *72*, 153403.
12. Chandrakumar, K. R. S.; Ghosh, S. K. Alkali-Metal-Induced Enhancement of Hydrogen Adsorption in C_{60} Fullerene: An *ab Initio* Study. *Nano Lett.* **2008**, *8*, 13–19.
13. Yildirim, T.; Ciraci, S. Titanium-Decorated Carbon Nanotubes as a Potential High-Capacity Hydrogen Storage Medium. *Phys. Rev. Lett.* **2005**, *94*, 175501.
14. Sun, Q.; Wang, Q.; Jena, P.; Kawazoe, Y. Clustering of Ti on a C_{60} Surface and Its Effect on Hydrogen Storage. *J. Am. Chem. Soc.* **2005**, *127*, 14582–14583.
15. Ishiharaa, T.; Nakasua, M.; Yasudab, I.; Matsumoto, H. Preparation of Si−Carbon Nanotube Composite by Decomposition of Tetramethylsilane (TMS) and Its Hydrogen Storage Property. *Sci. Technol. Adv. Mater.* **2006**, *7*, 667–671.
16. Wu, X. J.; Gao, Y.; Zeng, X. C. Hydrogen Storage in Pillared Li-Dispersed Boron Carbide Nanotubes. *J. Phys. Chem. C* **2008**, *112*, 8458–8463.
17. Lan, J.; Cheng, D.; Cao, D.; Wang, W. Silicon Nanotube as a Promising Candidate for Hydrogen Storage: From the First Principle Calculations to Grand Canonical Monte Carlo Simulations. *J. Phys. Chem. C* **2008**, *112*, 5598–5604.
18. Lee, J. B.; Lee, S. C.; Lee, S. M.; Kim, H. Hydrogen Adsorption Characteristics of Li-Dispersed Silica Nanotubes. *Chem. Phys. Lett.* **2007**, *436*, 162–166.
19. Karttunen, A. J.; Linnolahti, M.; Pakkanen, T. A. Icosahedral Polysilane Nanostructures. *J. Phys. Chem. C* **2007**, *111*, 2545–2547.
20. Zhang, D.; Ma, C.; Liu, C. Potential High-Capacity Hydrogen Storage Medium: Hydrogenated Silicon Fullerenes. *J. Phys. Chem. C* **2007**, *111*, 17099–17103.
21. Barman, S.; Sen, P.; Das, G. P. Ti-Decorated Doped Silicon Fullerene: A Possible Hydrogen-Storage Material. *J. Phys. Chem. C* **2008**, *112*, 19963–19968.
22. Furukawa, H.; Yaghi, O. M. Storage of Hydrogen, Methane, and Carbon Dioxide in Highly Porous Covalent Organic Frameworks for Clean Energy Applications. *J. Am. Chem. Soc.* **2009**, *131*, 8875–8883.
23. Cao, D.; Lan, J.; Wang, W.; Smit, B. Lithium-Doped 3D Covalent Organic Frameworks: High-Capacity Hydrogen Storage Materials. *Angew. Chem., Int. Ed.* **2009**, *48*, 4730–4733.
24. Kresse, G.; Hafner, J. *Ab Initio* Molecular Dynamics for Liquid Metals. *Phys. Rev. B* **1993**, 558–561.
25. Kresse, G.; J., F. Efficient Iterative Schemes for *ab Initio* Total-Energy Calculations Using a Plane-Wave Basis Set. *Phys. Rev. B* **1996**, *54*, 11169–11186.
26. Perdew, J. P.; Wang, Y. Accurate and Simple Analytic Representation of the Electron-Gas Correlation Energy. *Phys. Rev. B* **1992**, *45*, 13244–13249.
27. Vanderbilt, D. Soft Self-Consistent Pseudopotentials in a Generalized Eigenvalue Formalism. *Phys. Rev. B* **1990**, *41*, 7892–7895.
28. Kresse, G.; Hafner, J. Norm-Conserving and Ultrasoft Pseudopotentials for First-Row and Transition Elements. *J. Phys.: Condens. Matter* **1994**, *6*, 8245–8257.
29. Frenkel, D.; Smit, B. *Understanding Molecular Simulation*, 2nd ed.; Academic Press: San Diego, CA, 2002.
30. Xiang, Z. H.; Lan, J. H.; Cao, D. P.; Shao, X. H.; Wang, W. C.; Broom, D. Hydrogen Storage in Mesoporous Polymer Frameworks: Experiment and Simulation. *J. Phys. Chem. C* **2009**, *113*, 15106–15109.